PHYSICAL REVIEW A **87**, 042114 (2013)

# Resonant states for complex potentials and spectral singularities

Lorea Chaos-Cador[1,*] and Gastón García-Calderón[2,†]
[1] *Universidad Autónoma de la Ciudad de México, Prolongación San Isidro 151, 09790 México, Distrito Federal, Mexico*
[2] *Instituto de Física, Universidad Nacional Autónoma de México, Apartado Postal 20 364, 01000 México, Distrito Federal, Mexico*

(Received 11 October 2012; revised manuscript received 13 February 2013; published 22 April 2013)

We consider the analytical properties of the outgoing Green's function for complex potentials of finite range to study the relationship between its residues at the complex poles, the resonant states, and the spectral singularities of continuum wave functions. We obtain that the resonant state corresponding to a spectral singularity is a well-defined function, which we call the *spectral singularity resonant function*, and find a general expression that yields the position of the spectral singularity on the real wave number axis in terms of the imaginary part of the complex potential and the spectral singularity resonant function. We derive an analytical expression for continuum wave solutions as an expansion in terms of resonant states and the corresponding expression near a spectral singularity. Our findings are illustrated by considering an imaginary $\delta$-shell potential for $s$ waves.

DOI: 10.1103/PhysRevA.87.042114 PACS number(s): 03.65.Ca, 03.65.Xp

## I. INTRODUCTION

Spectral singularities correspond to points that may appear in the continuous spectra of open quantum systems involving complex potentials, where a continuum wave solution to the Schrödinger equation of the problem becomes singular. Some authors consider this situation to be a mathematical obstruction for the completeness of the continuum solutions [1]. See, however, Ref. [2] for a different conclusion. A consequence of the above is that the scattering coefficients become infinite at these spectral values [1,3]. They were mainly studied by mathematicians in the 1950s and 1960s [4–6] but in recent years have attracted the attention of investigations on the properties of $\mathcal{PT}$-symmetric and non-$\mathcal{PT}$-symmetric scattering potentials [7–9].

In recent work, Mostafazadeh [7,10] called the attention to the relationship of spectral singularities with resonant poles having a vanishing width. However, Mostafazadeh did not elaborate further on this appealing relationship. Spectral singularities have also been considered in other model complex potentials [11,12]. It worth mentioning work referring to the possible application of spectral singularities in waveguide physics [1,10,13].

In this work we generalize the formalism of resonant states [14,15] to complex potentials to investigate the relationship of resonant states and its corresponding poles with spectral singularities. We also derive exact analytical expressions for the expansion of the continuum wave solutions to the Schrödinger equation of the problem in terms of resonant states on the half-line and find the corresponding approximate expressions close to a spectral singularity.

In general, for real potentials, resonant states correspond to solutions to the Schrödinger equation which at large distances consist of purely outgoing waves. This implies that the corresponding energy eigenvalues are complex and therefore that the amplitude of the resonant function increases exponentially in space. A consequence of the above is that the usual rules concerning normalization, orthogonality, and completeness do not apply. Resonant states were introduced in quantum mechanics by Gamow in his studies on $\alpha$ decay in nuclei and constituted, in spite of the above apparent limitations, one of the first successful applications in the early days of quantum mechanics to tunneling phenomena [16,17]. Later on, resonant states were considered by Siegert [18] to derive a dispersion formula for nuclear reactions and by Humblet and Rosenfeld, who developed a formalism of nuclear reactions based on **S**-matrix resonant expansions [19]. It is worth pointing out that those expansions require only to know the resonant function at a given spatial point, usually the cutoff potential radius, and as a consequence the amplitude of the corresponding resonant states remains finite. Subsequent work addressed the issues of normalization and completeness of resonant states and led to a number of related approaches [14,20–22]. Our work is based on the analytical properties of the outgoing Green's function of the problem [23] and constitutes a description of resonant processes where the issues of normalization and completeness have been satisfactorily solved [14,15]. It provides an exact analytical description of transient phenomena in scattering [24,25] and for the exponential and nonexponential regimes of quantum decay [26–29]. Since the outgoing Green's function is a single-valued function of the wave number $k$, our analysis is given in terms of this variable and its extension to the complex $k$ plane and not on the energy $E = (\hbar^2/2m)k^2$, which requires of two Riemann energy sheets [12,30].

It might be of interest to some readers to mention a line of research where resonant states (named Gamow states) are considered as objects in a rigged Hilbert space formulation which characterizes itself because it modifies one of the axioms of quantum mechanics [31]. In recent years, however, that approach has become controversial [32,33]. Our approach differs in many respects from the Bohm-Gadella rigged Hilbert approach, as for example the normalization condition and the resonant expansions, which in our case refer to $r \in (0,a)$ and in theirs encompass the full half line $r \in (0,\infty)$. To the best of our knowledge the rigged-Hilbert space formulations have not been concerned with the subject of the present work.

All the works on resonant states mentioned above refer to real potential interactions and hence do not provide the conditions for the existence of spectral singularities, which require, as pointed out above, complex or purely imaginary

---

[*] lorea@ciencias.unam.mx

[†] gaston@fisica.unam.mx

potentials [1]. One finds in the literature a number of works that have addressed the issue of the complex poles for the **S** matrix on the $k$ plane for complex potentials in three dimensions [34–36] and also works considering the notion of resonant state to express the inelastic width, respectively, in one and two dimensions [37,38]. See Ref. [39] for a review on complex absorbing potentials.

The paper is organized as follows. In Sec. II, we discuss the extension of the formalism of resonant states to complex potentials and derive an expression of the spectral singularity in terms of resonant functions. Section III discusses the relationship of continuum wave functions with the outgoing Green's function and presents an expression relating a continuum wave solution with a resonant state close to a spectral singularity. Section IV discusses in detail the example of the distribution of the complex poles to the outgoing Green's function for both purely absorptive and emissive $\delta$-shell potentials for $s$ waves. Finally, Sec. V gives the concluding remarks.

## II. RESONANT STATES FOR COMPLEX POTENTIALS

For the sake of simplicity, we restrict the discussion to $s$ waves in spherical symmetric potentials in three dimensions. This, however, is equivalent to a discussion on the half line $r \in (0,\infty)$. The analytic continuation of the solutions to the Schrödinger equation to complex values of the wave number $k$, where $k = [2mE]^{1/2}/\hbar$, with $E$ the energy and $m$ the mass of the particle, depends on general properties on the behavior of the interaction potential as a function of distance. For well-behaved potentials (nonsingular at the origin) that vanish exactly beyond a finite distance, the outgoing Green's function to the problem $G^+(r,r';k)$ is a meromorphic function in the whole complex $k$ plane [23,40]. Although most work on resonant states refers to potential interactions that are real, the above result holds also if the potential is complex [23].

The outgoing Green's function to the problem is the relevant quantity to study the properties of resonant states. It satisfies the equation

$$G''^{+}(r,r';k) + [k^2 - U(r)]G^+(r,r';k) = (2m/\hbar^2)\delta(r - r'), \tag{1}$$

with boundary conditions

$$G^+(0,r';k) = 0, \quad [G'^{+}(r,r';k)]_{r=a} = ikG^+(a,r';k), \tag{2}$$

where $G''^{+}$ and $G'^{+}$ denote, respectively, the second and first partial derivatives of $G^+$ with respect to $r$ and the interaction potential $U(r)$ is defined by

$$U(r) = (2m/\hbar^2)[V_0(r) \mp iW(r)] = \mathcal{V}_0(r) \mp i\mathcal{W}(r). \tag{3}$$

We consider that $V_0(r)$ and $W(r)$ are potentials that vanish beyond the finite interval $r = a$, namely, $V(r) = 0, r > a$ and $W(r) = 0, r > a$. We define $W(r)$ as a positive definite function and hence the minus sign in (3) indicates that the imaginary part of the potential is absorptive and, respectively, that the plus sign corresponds to a process of emission by the potential. It is worth noticing that the absorptive potential preserves the causality condition [34,41,42], whereas this is not so for emission by the potential.

The outgoing Green's function may be written as [23]

$$G^+(r,r';k) = -(2m/\hbar^2)\,\frac{\phi(k,r_<)f_+(k,r_>)}{J_+(k)}, \tag{4}$$

where the notation $r_<$ means the smaller of $r$ and $r'$ and $r_>$ means the larger. The functions $\phi(k,r)$ and $f_\pm(k,r)$ stand, respectively, for the *regular* and *irregular* solutions to the Schrödinger equation to the problem

$$\psi''(k,r) + [k^2 - U(r)]\psi(k,r) = 0, \tag{5}$$

obeying the boundary conditions

$$\phi(k,0) = 0, \quad [\phi'(k,r)]_{r=0} = 1; \quad \lim_{r\to\infty} f_\pm(k,r) = e^{\pm ikr}, \tag{6}$$

and $J_\pm(k)$ refer to the Jost functions defined by the Wronskian $J_\pm(k) = W[f_\pm,\phi] = (f_\pm(k,r)\phi'(k,r) - f'_\pm(k,r)\phi(k,r))$. In the above expressions the prime and double prime denote, respectively, the first and second derivatives with respect to the variable $r$. We adopt such a notation from now onwards.

As is well known the two solutions $f_+(k,r)$ and $f_-(k,r)$ of (5) are linearly independent and hence the *regular* solution may be expressed as a linear combination of them [23],

$$\phi(k,r) = \frac{1}{2ik}[J_-(k)f_+(k,r) - J_+(k)f_-(k,r)]. \tag{7}$$

It is of interest to write the integral representation of the Jost functions $J_\pm(k)$,

$$J_\pm(k) = 1 + k^{-1}\int_0^\infty \sin kr\, U(r) f_\pm(k,r)\,dr. \tag{8}$$

The functions $\phi(k,r)$ and $f_\pm(k,r)$ are entire functions of $k$ and hence the poles of the outgoing Green's functions correspond to the zeros of $J_+(k)$. There is an infinite number of them seated on the complex $k$ plane [40]. These poles are, except in special cases that depend on specific combination of the parameters of the potential, simple, and we assume that this is the case here. For real potentials, it follows from time-reversal considerations that the complex poles lie on the lower half of the $k$ plane and are distributed symmetrically with respect to the imaginary $k$ axis. Thus, for a given pole $\kappa_n$ seated on the fourth quadrant, there is a pole $\kappa_{-n} = -\kappa_n^*$ seated on the third quadrant. One may also find, depending on the potential parameters, that there might be a finite number of purely imaginary poles located on the imaginary $k$ axis. Those situated on the positive imaginary axis correspond to bound states, whereas those on the negative imaginary axis correspond to antibound sates [15,19,23]. As a function of the potential parameters, the poles follow trajectories on the complex $k$ plane. In particular, these trajectories reflect the symmetry mentioned above. Adding an imaginary part to the potential destroys the above symmetry and, hence, the trajectory that follows a pole $\kappa_n$ on the fourth quadrant of the $k$ plane ceases to be related by time-reversal invariance to that of the pole $\kappa_{-n}$. For both real and complex potentials with a negative imaginary part, causality prevents the presence of complex poles on the first quadrant of the complex $k$ plane [34,41,42]. This ceases to hold for complex potentials with a positive imaginary part [34].

Resonant states follow from the residues at the complex poles of the outgoing Green's function to the problem. As shown in Appendix A, the derivation of the residue for real potentials [14,15] follows also for complex potentials. The residue $r_n = \lim_{k\to\kappa_n}(k-\kappa_n)G^+(r,r';k)$ at a complex pole $\kappa_n$ seated on the complex $k$ plane is given by

$$r_n = (2m/\hbar^2)\frac{u_n(r)u_n(r')}{2\kappa_n}, \tag{9}$$

provided resonant states are normalized according to the condition

$$\int_0^a u_n^2(r)\,dr + i\frac{u_n^2(a)}{2\kappa_n} = 1. \tag{10}$$

The resonant functions $u_n(r)$ satisfy the Schrödinger equation,

$$u''_n(r) + \left[\kappa_n^2 - \{\mathcal{V}_0(r) \mp i\mathcal{W}(r)\}\right]u_n(r) = 0, \tag{11}$$

and in general obey purely outgoing boundary conditions at $r = a$, namely,

$$u_n(0) = 0, \quad [u'_n(r)]_{r=a} = i\kappa_n u_n(a), \tag{12}$$

where we define

$$\kappa_n = \alpha_n - i\beta_n. \tag{13}$$

Consequently, the complex energy eigenvalue reads

$$E_n = \hbar^2\kappa_n^2/2m = \mathcal{E}_n - i\Gamma_n/2, \tag{14}$$

where $\mathcal{E}_n$ and $\Gamma_n$ represent, respectively, the energy position and the energy width of the resonance. Using (13) in (14), one obtains the useful relationships

$$\mathcal{E}_n = \frac{\hbar^2}{2m}\left(\alpha_n^2 - \beta_n^2\right), \quad \Gamma_n = \frac{\hbar^2}{2m}4\alpha_n\beta_n. \tag{15}$$

As shown in Appendix B the outgoing Green's function to the problem may be expanded in terms of resonance states in a similar fashion as considered for real potentials [14,15]. It reads

$$G^+(r,r';k) = (2m/\hbar^2)\sum_{n=-\infty}^{\infty}\frac{u_n(r)u_n(r')}{2\kappa_n(k-\kappa_n)}, \quad (r,r')^\dagger \leqslant a, \tag{16}$$

where $(r,r')^\dagger \leqslant a$ denotes that $r$ and $r'$ are smaller than the interaction radius $a$ or $r = a$ with $r' < a$ and vice versa. Substitution of (16) into the equation for $G^+(r,r';k)$ given by (1), after addition and subtraction of $(k^2-\kappa_n^2)G^+(r,r';k)$, yields

$$\sum_{n=-\infty}^{\infty}\frac{k+\kappa_n}{2\kappa_n}u_n(r)u_n(r') = \delta(r-r'), \quad (r,r')^\dagger \leqslant a. \tag{17}$$

In order to satisfy (17), the following relationships must be obeyed,

$$\frac{1}{2}\sum_{n=-\infty}^{\infty}u_n(r)u_n(r') = \delta(r-r'), \quad (r,r')^\dagger \leqslant a, \tag{18}$$

which correspond to a closure relationship, and the sum rule

$$\sum_{n=-\infty}^{\infty}\frac{u_n(r)u_n(r')}{\kappa_n} = 0, \quad (r,r')^\dagger \leqslant a. \tag{19}$$

Noticing that

$$\frac{1}{2\kappa_n(k-\kappa_n)} = \frac{1}{2k}\left[\frac{1}{k-\kappa_n} + \frac{1}{\kappa_n}\right] \tag{20}$$

makes it possible to write the expansion of $G^+(r,r';k)$, in view of (19), as

$$G^+(r,r';k) = (2m/\hbar^2)\frac{1}{2k}\sum_{n=-\infty}^{\infty}\frac{u_n(r)u_n(r')}{k-\kappa_n}, \quad (r,r')^\dagger \leqslant a. \tag{21}$$

Now substitution of (21) into (1) and proceeding in a similar fashion as above yields the additional sum rule

$$\sum_{n=-\infty}^{\infty}u_n(r)u_n(r')\kappa_n = 0, \quad (r,r')^\dagger \leqslant a. \tag{22}$$

It is worth mentioning that an arbitrary function $F(r)$ may be expanded in terms of resonant states along the region $(r,r')^\dagger \leqslant a$ using the closure relationship given by Eq. (18), so one may write

$$F(r) = \frac{1}{2}\sum_{n=-\infty}^{\infty}C_n u_n(r), \quad r \leqslant a, \tag{23}$$

where

$$C_n = \int_0^a F(r)u_n(r)\,dr. \tag{24}$$

An interesting example of a choice $F(r)$ has been given by Exner and Fraas [43], who considered $F(r)$ to be a constant within the interaction region of a $\delta$-shell potential that yields a highly irregular, most likely fractal, behavior for the nondecay probability.

If the function $F(r)$ is normalized along the internal region, then multiplying (23) by $F^*(r)$ and performing an integration from $r = 0$ to $r = a$ yields

$$\frac{1}{2}\sum_{n=-\infty}^{\infty}C_n\bar{C}_n = 1, \tag{25}$$

where

$$\bar{C}_n = \int_0^a F^*(r)u_n(r)\,dr. \tag{26}$$

The coefficients $C_n$ and $\bar{C}_n$ cannot be interpreted as probability amplitudes since they are complex quantities. This is related to the occurrence in all these equations of the square of the resonant eigenfunctions and not of their square modulus. Nevertheless, as exemplified in Sec. IV D, since (25) adds up to unity, each real term in that sum yields a measure of the strength of the expanded function for the corresponding resonant state.

### A. Distribution of poles on the *k* plane and spectral singularities

Here we find it convenient to discuss separately the cases of absorption and emission.

#### *1. Absorption*

Here we refer to the potential $\mathcal{V}_0(r) - i\mathcal{W}(r)$. Using (14), one may write the time-dependent resonant state function as

$$u_n(r,t) = u_n(r)e^{-i\mathcal{E}_n t/\hbar}e^{-\Gamma_n t/\hbar}. \tag{27}$$

It is of interest to notice that the variation with time of the total probability density along the internal region of the potential satisfies the continuity equation. Using (27), one obtains immediately

$$\frac{d}{dt}(I_n e^{-\Gamma_n t/\hbar}) = -\mathcal{J}_n(a,t) - \frac{\hbar}{m}\, Y_n e^{-\Gamma_n t/\hbar}, \tag{28}$$

where $I_n$ reads

$$I_n = \int_0^a |v_n(r)|^2\, dr, \tag{29}$$

$\mathcal{J}_n(a,t) = \mathcal{J}_n(a)\exp(-\Gamma_n t/\hbar)$ stands for the probability current with $\mathcal{J}_n(a)$ given by

$$\mathcal{J}_n(a) = \frac{\hbar}{m}\mathrm{Im}\left[v_n^*(r)\frac{d}{dr}v_n(r)\right]_{r=a}, \tag{30}$$

and

$$Y_n = \int_0^a |v_n(r)|^2 \mathcal{W}(r)\, dr. \tag{31}$$

Using the boundary condition at $r = a$ given in (12) in (30) makes it possible to write $\mathcal{J}_n(a,t)$ as

$$\mathcal{J}_n(a,t) = \frac{\hbar}{m}\alpha_n |v_n(a)|^2 e^{-\Gamma_n t/\hbar}. \tag{32}$$

Hence, using (32) in (28), in view of (15), yields

$$\alpha_n\left[|v_n(a)|^2 - 2\beta_n I_n + \frac{Y_n}{\alpha_n}\right] = 0. \tag{33}$$

Equation (33) inform us that if $\alpha_n \neq 0$ then

$$\beta_n = \frac{1}{2I_n}\left[|v_n(a)|^2 + \frac{Y_n}{\alpha_n}\right]. \tag{34}$$

From (34) we can learn about some general features of the distribution of the complex poles $\kappa_n$ on the complex $k$ plane in the presence of an absorptive potential.

Let us first consider the case for values of $\mathrm{Re}\, k > 0$, i.e., with poles characterized by $\alpha_n > 0$, which refers to the quadrants I and IV of the $k$ plane. Then it follows by inspection of the right-hand side of Eq. (34), recalling that we have defined $\kappa_n$ as $\kappa_n = \alpha_n - i\beta_n$, that $\beta_n > 0$, which means that there are no complex poles that may seat on the first quadrant of the $k$ plane. This is in accordance with the requirements of causality [34,41,42]. The above implies that in this case the complex poles are distributed only on the fourth quadrant, as occurs also for real potentials. Moreover, Eq. (34) also inform us that for complex potentials there are no poles seated on the imaginary $k$ axis. This requires that $\alpha_n = 0$ and one sees from (34) that then $\beta_n$ goes to infinity.

Next, let us consider the case with $\mathrm{Re}\, k < 0$, which corresponds to poles having $\alpha_n < 0$ and refers to quadrants II and III of the $k$ plane. Then one sees, by inspection of Eq. (34), that three situations may occur depending on whether the term within brackets on the right-hand side of (34) is, respectively, larger, smaller, or equal to zero. For the first two situations, the pole $\kappa_n$ seats, respectively, on the second or on the third quadrant of the complex $k$ plane. More interestingly, however, is the situation where the bracket vanishes identically, because then it means that $\beta_n = 0$. This situation corresponds to a spectral singularity [1], namely, to the situation of a pole with a vanishing width. Let us denote this solution by the subscript $s$; that is, from Eq. (34), $\beta_s = 0$ implies that

$$\alpha_s = -\frac{\int_0^a |v_s(r)|^2 \mathcal{W}(r)\, dr}{|v_s(a)|^2}. \tag{35}$$

The above equation provides an expression for the position of the spectral singularity in terms of both the imaginary part of the complex potential $\mathcal{W}$ and the function $v_s(r)$ that may be named *spectral singularity resonant function*. Notice that in the absence of an imaginary potential contribution, i.e., for a real potential, the solution $\alpha_s$ does not exist. The above considerations permit one to write, using (15), (35), and (27), the time-dependent spectral singularity resonant function as

$$v_s(r,t) = v_s(r)e^{-i\mathcal{E}_s t/\hbar}, \tag{36}$$

where $\mathcal{E}_s = (\hbar^2/2m)\alpha_s^2$. We recall that $v_s(r)$ is normalized according to Eq. (10). Notice that for $r > a$, it behaves as $v_s(r) \sim \exp(-i\alpha_s r)$.

It is worth mentioning that for the complex poles seated on the second quadrant, which are located at positions $\kappa_n = -\alpha_n + i\beta_n$, the corresponding resonant functions are square integrable, i.e., for $r > a$, $v_n(r) \sim \exp(-i\alpha_n r)\exp(-\beta_n r)$. In this case, as for bound states in real potentials, the normalization condition given by Eq. (10) may be expressed as an integral over the whole space.

### 2. *Emission*

Emission follows by considering the plus sign in the imaginary part of the complex potential in Eq. (11). Hence, the procedure considered above involving the continuity equation leads to an expression for $\beta_n$ that differs from Eq. (34) precisely in the change of sign of $Y_n$, namely,

$$\beta_n = \frac{1}{2I_n}\left[|v_n(a)|^2 - \frac{Y_n}{\alpha_n}\right]. \tag{37}$$

It follows immediately by inspection of Eq. (37), that the case for emission with values $\mathrm{Re}\, k > 0$, i.e., with $\alpha_n > 0$, corresponds exactly with the discussion given for the absorptive case with values $\mathrm{Re}\, k < 0$ and similarly, that the case for emission with values $\mathrm{Re}\, k > 0$, i.e., with $\alpha_n < 0$, corresponds exactly with the absorptive case with $\mathrm{Re}\, k > 0$.

It is worth stressing two points. First, for absorption, the spectral singularity lies along the negative real $k$ axis, as specified by Eq. (35), whereas for emission, the spectral singularity seats on the positive real $k$ axis,

$$\alpha_s = \frac{\int_0^a |v_s(r)|^2 \mathcal{W}(r)\, dr}{|v_s(a)|^2}. \tag{38}$$

Second, for emission there appear poles seated on the first quadrant of the $k$ plane, characterized by values $\kappa_n = \alpha_n + i\beta_n$, with $(\alpha_n,\beta_n) > 0$, that yield time-dependent solutions that grow exponentially with time.

## III. EXPANSION OF CONTINUUM WAVE SOLUTIONS IN RESONANT STATES

The continuum solutions $\psi^+(k,r)$ for the complex potential defined by (3) satisfy the Schrödinger equation

$$\psi''^+(k,r) + [k^2 - U(r)]\psi^+(k,r) = 0, \tag{39}$$

with the boundary conditions

$$\psi^+(k,0) = 0, \tag{40}$$

and

$$\psi^+(k,r) = \frac{i}{2}[e^{-ikr} - \mathbf{S}(k)e^{ikr}], \quad r \geqslant a, \tag{41}$$

where $\mathbf{S}(k)$ stands for the $\mathbf{S}$ matrix to the problem defined by

$$\mathbf{S}(k) = \frac{J_-(k)}{J_+(k)}. \tag{42}$$

Clearly, in the absence of a potential $\mathbf{S}(k) = 1$ and then the solution behaves as the free solution $\psi_f^+(k,r) = \sin(kr)$.

It is well known that the Jost function satisfies the relationship [23]

$$J_+^*(k^*,U^*) = J_-(k,U), \tag{43}$$

where $U$ stands for the complex potential defined by (3). Using (42) and (43) leads to the properties

$$\mathbf{S}(k)\mathbf{S}(-k) = 1, \tag{44}$$

$$\mathbf{S}^*(k,U)\mathbf{S}(k^*,U^*) = 1, \tag{45}$$

and using the above two expressions,

$$\mathbf{S}^*(-k^*,U^*) = \mathbf{S}(k,U). \tag{46}$$

From (44) one immediately sees that if $k$ is a pole of $\mathbf{S}$ then $-k$ is a zero of that function. As pointed out in Ref. [34], this result is independent of whether the potential is or is not complex and it is only a consequence of the spherical symmetry of the potential. Equation (46) is interesting because it informs us that if $k$ is a pole or zero of $\mathbf{S}(k,U)$, then $-k^*$ will be a pole or zero of $\mathbf{S}(k,U^*)$. This implies that for a complex potential the usual mirror symmetry with respect to the imaginary $k$ axis which holds for real potentials breaks down. The poles and zeros of $\mathbf{S}(k,U)$ and those corresponding to $\mathbf{S}(k,U^*)$ lie distributed symmetrically with respect to the imaginary $k$ axis. As a consequence, as was obtained in Sec. II A, knowing the position of the poles, say for the absorptive case, makes it possible to determine immediately the poles that correspond to the emissive case.

It is well known that the continuum solution $\psi^+(k,r)$ may be written in terms of the regular solutions $\phi(k,r)$ as [15]

$$\psi^+(k,r) = \frac{k\phi(k,r)}{J_+(k)}. \tag{47}$$

Clearly, from Eqs. (41) and (42), one sees that at a spectral singularity $k = k_s$, both $\mathbf{S}(k)$ and $\psi^+(k,r)$ diverge to infinity since $J_+(k_s) = 0$.

A relationship between the continuum wave solution and the outgoing Green's function follows using Eqs. (1) and (47), namely [44,45],

$$\psi^+(k,r) = -(\hbar^2/2m)\, k\, G^+(a,r;k)e^{-ika}, \quad r \leqslant a. \tag{48}$$

Using Eq. (16) one may write the continuum wave solution along the internal interaction region as an expansion in resonant states [44],

$$\psi^+(k,r) = -\sum_{n=-\infty}^{\infty} \frac{k u_n(a)e^{-ika}}{2\kappa_n(k-\kappa_n)} u_n(r), \quad r < a. \tag{49}$$

For values of $k$ close to a spectral singularity, $k \approx \kappa_s$, one may write $\psi^+(k,r)$ using (49) as

$$\psi^+(k,r) \approx -\frac{k u_s(a)e^{-ika}}{2\kappa_s(k-\kappa_s)} u_s(r), \quad r < a. \tag{50}$$

Equation (50) yields a relationship between the continuum wave solution and the spectral singularity resonant function in the vicinity of the spectral singularity $\kappa_s$ and shows explicitly that $\psi^+(k,r) \to \infty$ as $k \to \kappa_s$.

Alternatively, using the closure relation (18), one may expand $\psi^+(k,r)$ along the internal region as [44]

$$\psi^+(k,r) = \frac{1}{2}\sum_{n=-\infty}^{\infty} C_n(k)u_n(r), \quad r < a, \tag{51}$$

with

$$C_n(k) = \int_0^a \psi^+(k,r)u_n(r)\,dr. \tag{52}$$

Notice that either (49) or (51) establishes an exact analytical relationship between continuum wave solutions and the resonant states of the problem.

Along the external interaction region, $r \geqslant a$, the resonant expansion of $\psi^+(k,r)$ follows by expanding $\mathbf{S}(k)$ in (41). This has been discussed by Humblet and Rosenfeld, who considered the Mittag-Leffler theorem to expand $\mathbf{S}(k)$ [19]. This yields, in addition to a discrete sum, an integral contribution that, however, is not necessarily negligible [45]. A more appropriate resonant expansion may be obtained via the outgoing Green's function. Substitution of (41) at $r = a$ into (48) makes it possible to write

$$\mathbf{S}(k) = [1 - 2ik(\hbar^2/2m)G^+(a,a;k)]e^{-2ika}. \tag{53}$$

Although $G^+(a,a;k)$ diverges as $|k| \to \infty$ along the $k$ plane, it does so linearly with $k$ [44,46], and hence a convergent resonant expansion with two subtraction terms may be obtained using the Cauchy theorem [45],

$$G^+(a,a;k) = G^+(a,a;0) + k\dot{G}^+(a,a;0) + (2m/\hbar^2)k^2 \sum_{n=-\infty}^{\infty} \frac{u_n^2(a)}{2\kappa_n^3(k-\kappa_n)}, \tag{54}$$

where $\dot{G}^+(a,a;0)$ denotes the derivative of $G^+(a,a;k)$ with respect to $k$ evaluated at $k = 0$. Substitution of (54) into (53) and the resulting expression into (41) provides a convergent resonant expansion plus a nonresonant contribution for $\psi^+(k,r)$ along the external region, namely,

$$\psi^+(k,r) = -\sum_{n=-\infty}^{\infty} \frac{k^3 u_n^2(a)e^{-2ika}}{2\kappa_n^3(k-\kappa_n)} e^{ikr} + (\hbar^2/2m)Q(k,r), \quad r \geqslant a, \tag{55}$$

where the nonresonant contribution $Q(k,r)$ reads $Q(k,r) = (2m/\hbar^2)(i/2)[\exp(-ikr) - \exp(-2ika)\exp(ikr)] - k[G^+(a,a;0) + k\dot{G}^+(a,a;0)]\exp(-2ika)\exp(ikr)$.

Again, for values of $k$ very close to a spectral singularity located at $\kappa_s$, we may write the continuum wave function along the external region as

$$\psi^+(k,r) \approx -\frac{k^3 u_s^2(a)e^{-2ika}}{2\kappa_s^3(k-\kappa_s)} e^{ikr}, \quad r \geqslant a, \tag{56}$$

which exhibits explicitly that the continuum wave solution along the external region diverges at $k = \kappa_s$.

It should be stressed, as shown by Eqs. (49) and (55), that one requires to know resonant functions only in the interval $0 \leqslant r \leqslant a$ to characterize the continuum wave solutions along the full interval $(0,\infty)$.

It is worth mentioning some recent work on the full line that shows that by using an auxiliary function that is very easy to calculate one may obtain a purely discrete expansion involving resonant states for the reflection amplitude, which is the full-line counterpart of $\mathbf{S}(k)$ [47]. That work has been relevant for an exact analytical description of quantum transients in one-dimensional scattering [48].

## IV. EXAMPLE

As an example, we refer in detail to the case of a purely *absorptive* potential. Hence, from Eq. (3), $\mathcal{W}(r) = (2m/\hbar^2)W(r)$ and we choose the $\delta$-shell potential $W(r) = (\hbar^2/2m)b\delta(r-a)$, so we may write

$$U(r) = -i\mathcal{W}(r) = -ib\,\delta(r-a), \tag{57}$$

where the intensity $b > 0$. For simplicity of the discussion we take as units $\hbar = 2m = 1$. Clearly, the case of an *emissive* $\delta$ potential follows by changing the sign in (57). We refer to this case in Sec. IV D. Our aim is to obtain the set of complex poles $\{\kappa_n\}$ and resonant states $\{u_n(r)\}$ for this problem and, in particular, for the spectral singularities.

Substitution of (57) into (11), in view of the boundary conditions (12), makes it possible to write the solution to the problem as

$$u_n(r) = \begin{cases} A_n \sin(\kappa_n r), & r \leqslant a, \\ B_n\, e^{i\kappa_n r}, & r \geqslant a. \end{cases} \tag{58}$$

It follows immediately by continuity of the solutions and the discontinuity of its derivatives with respect to $r$ (due to the $\delta$ interaction), at the radius $r = a$, that the values of $\kappa_n$ are solutions to the equation

$$2\kappa_n - b\,(e^{2i\kappa_n a} - 1) = 0, \tag{59}$$

which correspond precisely to the zeros of the Jost function of the problem as may be easily verified by substitution of (57) into the expression given by (8), namely,

$$J_+(k) = 1 - \frac{b}{2k}\,(e^{2ika} - 1). \tag{60}$$

Using (60) and (42) we may write the $\mathbf{S}$ matrix to the problem as

$$\mathbf{S}(k) = -\frac{2k + b\,(e^{-2ika} - 1)}{2k - b\,(e^{2ika} - 1)}. \tag{61}$$

### A. Distribution of the poles on the *k* plane

Equation (59) possesses an infinite number of solutions which unfortunately cannot be obtained exactly in an analytical fashion. However, within certain limits to be discussed below, one may obtain approximate analytical solutions that may be used as an input in well-known iteration procedures, as the Newton-Raphson method [49], to obtain the solutions to a desired degree of approximation.

Since time-reversal invariance does not hold for a imaginary potentials, it is convenient to refer first to the solutions on the fourth quadrant of the $k$ plane. These solutions may be characterized by

$$\kappa_n = \alpha_n - i\beta_n, \tag{62}$$

with $n = 1,2,3,\ldots$ and $\alpha_n,\beta_n > 0$. Substitution of (62) into (59) leads to a couple of equations that may be written as

$$\frac{2\alpha_n + b}{b} = \cos(2\alpha_n a)\, e^{2\beta_b a} \tag{63}$$

and

$$-\frac{2\beta_n}{b} = \sin(2\alpha_n a)\, e^{2\beta_n a}. \tag{64}$$

Then, dividing (64) by (63) one gets

$$\tan(2\alpha_n a) = -\frac{2\beta_n}{2\alpha_n + b}, \tag{65}$$

and squaring and adding both (63) and (64) gives

$$\beta_n = \frac{1}{4a}\ln\left[\left(1 + \frac{2\alpha_n}{b}\right)^2 + \left(\frac{2\beta_n}{b}\right)^2\right]. \tag{66}$$

It is easily verified that in the limit $b \to \infty$, (65) and (66) give, respectively, $\tan(2\alpha_n a) = 0$ and $\beta_n = 0$. The solutions to the first equation are, of course, $\alpha_n = n\pi/a$ and correspond to quantum states trapped inside the region $0 < r < a$. This is peculiar because the potential is purely imaginary and absorptive. For very large but finite $b$, i.e., $b \gg 1$ one may write, in general,

$$\alpha_n = \frac{n\pi}{a} + \epsilon_n, \tag{67}$$

where $0 < \epsilon_n < n\pi/a$. Substitution of (67) into (65) leads to the following expression for $\epsilon_n$:

$$\epsilon_n = -\frac{1}{2a}\tan^{-1}\left(\frac{2\beta_n/b}{1 + 2\alpha_n/b}\right). \tag{68}$$

It is not difficult to see that if $b \gg n\pi$ one may substitute to first order $\alpha_n = n\pi/a$ in (68) and also if $b \gg \beta_n$ and $n\pi \gg \beta_n a$, one may write $\epsilon_n$ approximately as

$$\epsilon_n \approx -\frac{1}{a}\frac{\beta_n a}{ba}, \tag{69}$$

where $\beta_n a/ba \ll 1$. Noticing that $(2n\pi/ba) \gg (2\beta_n a/ba)$, one may use the above results into (66) to find the expression

$$\beta_n \approx \frac{1}{a}\frac{n\pi}{ba}. \tag{70}$$

Using (70) in (69) makes it possible to see that $\epsilon_n$ is indeed an extremely small quantity. Therefore, it follows that the approximate analytical solutions to Eq. (59) are given by

$$\kappa_n \approx \frac{n\pi}{a} - i\frac{1}{a}\frac{n\pi}{ba}, \tag{71}$$

where we recall that (71) holds provided $ba \gg 1$ and $ba \gg n\pi$, which correspond to poles lying very close to the real $k$ axis.

Changing $n \to -n$ in Eq. (71) yields a solution to Eq. (59) that lies on the second quadrant of the $k$ plane, namely,

$$\kappa_{-n} \approx -\frac{n\pi}{a} + i\frac{1}{a}\frac{n\pi}{ba}. \tag{72}$$

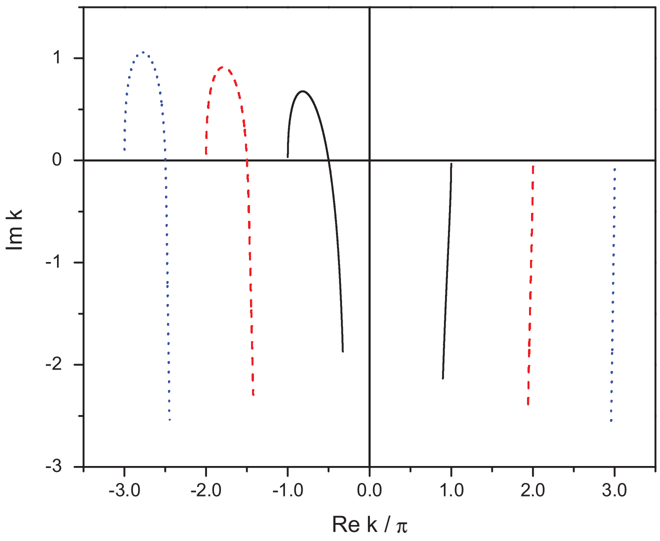

FIG. 1. (Color online) Plot of the trajectories of the complex poles $\kappa_n$ along the complex $k$ plane corresponding to a purely absorptive $\delta$-shell potential $U(r) = -ib\delta(r-a)$, with $a = 1$. For $b = \infty$ the poles lie at values $\kappa_n = \pm n\pi$, with $n = 1,2,3,\ldots$. As $b \to 0$, $\mathrm{Im}\,\kappa_n \to -\infty$. At the intensity values $b_s = (2s-1)\pi/2a$ one finds spectral singularities at the real pole positions $\alpha_s = -b_s$, $s = 1,2,3,\ldots$. See text.

One may use the approximate analytical solution (72) as an input in the Newton-Rapshon method [49] to evaluate the solutions with any degree of accuracy. In our case the method consists in solving by iteration the equation

$$\kappa_n^{r+1} = \kappa_n^r - \frac{J_+(\kappa_n^r)}{\dot{J}_+(\kappa_n^r)}, \tag{73}$$

where $r = 1,2,\ldots$, $J_+(k)$ is given by (60), and $\dot{J}_+(k)$ stands for the derivative of $J_+(k)$ with respect to $k$, namely, $\dot{J}_+(k) = 2[1 - iba\,\exp(2ika)]$. Once a pole has been calculated its trajectory along the $k$ plane may be obtained as a function of $b$. Denote this pole by $\kappa_n(b)$ and use it as an input in Eq. (73) for a slightly smaller value of $b - \delta b$. This leads to the new pole $\kappa_n(b-\delta b)$ and by repeating this procedure one then generates the trajectory that each pole follows on the $k$ plane.

Figure 1 illustrates the trajectories followed by the poles $\kappa_n$ and $\kappa_{-n}$ with $n = 1,2,3$. One sees that as $b$ diminishes, the poles on the second quadrant follow trajectories that eventually leads them to the third quadrant. In crossing the real $k$ axis, each of these poles attains a vanishing imaginary value that corresponds precisely to a spectral singularity. That occurs at distinct values of $b$ for each pole. On the other hand, in a similar fashion, one sees that the poles on the fourth quadrant follow trajectories that take them away from the real $k$ axis.

#### *1. Asymptotically large complex poles*

There is still another approximate analytical solution for the complex poles $\kappa_n$. This follows in the limit of very large poles. The former condition $ba \gg 1$ still holds, so the starting points of the approximation are Eqs. (66) and (68), onto which we impose the condition $n\pi \gg ba$. It is then easily seen that the approximate solution $\kappa_n$ for asymptotic large values of $n$ for poles seated on the fourth quadrant of the $k$ plane are

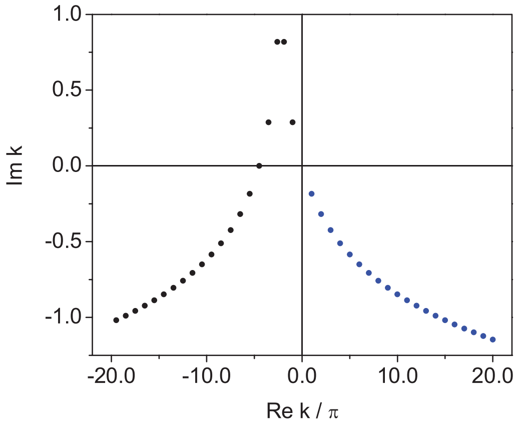

FIG. 2. (Color online) Plot of the distribution of the first 20 complex poles on the $k$ plane, corresponding to the purely absorptive $\delta$-shell potential $U(r) = -ib\delta(r-a)$ with $b = b_5 = 9\pi/2$ and $a = 1$, which yields a spectral singularity at $\alpha_5 = -b_5$. See text.

$$\kappa_n \approx \frac{n\pi}{a} - i\frac{1}{4a}\ln(2n)^2. \tag{74}$$

Changing $n \to -n$ yields now an approximate solution that seats on the third quadrant of the $k$ plane, namely,

$$\kappa_{-n} \approx -\frac{n\pi}{a} - i\frac{1}{4a}\ln(2n)^2. \tag{75}$$

The above solutions are rather interesting; they imply that at asymptotically large values of $n$ one seems to recover the condition for time-reversal invariance $\kappa_{-n} = -\kappa_n^*$. This deserves further investigation.

### B. Spectral singularities

In our simple example one may determine the distinct values of $b > 0$ at which the spectral singularities occur. We denote these solutions by the subindex $s$ and they follow immediately by substitution of $\kappa_n = \alpha_s$ into Eq. (59). This leads to the equations

$$2\alpha_s - b\cos(2\alpha_s a) + b = 0 \tag{76}$$

and

$$\sin(2\alpha_s a) = 0. \tag{77}$$

The solution to Eqs. (76) and (77) is of the form

$$\alpha_s = (2s-1)\pi/2a, \tag{78}$$

with $s = 1,2,3\ldots$, which holds provided the intensity $b$ acquires the values

$$\alpha_s = -b_s. \tag{79}$$

The above expression implies that for absorption, $\alpha_s$ is always seated on the negative real $k$ axis, and provides the value of the intensity of the $\delta$-shell potential to guarantee the existence of a spectral singularity for that potential. Equation (79) follows also from (35) since $\mathcal{W}(r) = b\,\delta(r-a)$.

Figure 2 exhibits the distribution of the first 20 poles of our problem for parameters $b_5 = 9\pi/2$ and $a = 1$. Notice that a spectral singularity occurs precisely at $\alpha_5 = -9\pi/2$. For that

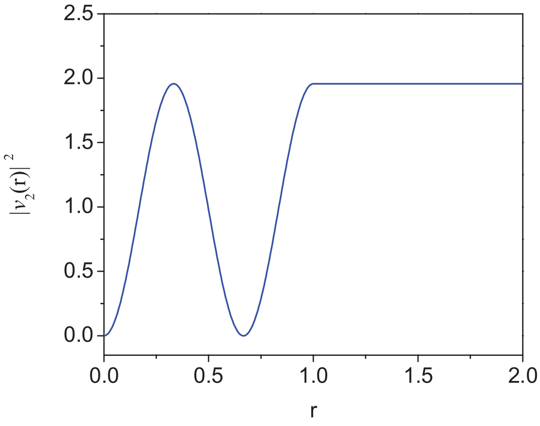

FIG. 3. (Color online) Plot of the probability density of the spectral singularity resonant function $|v_2(r)|^2$ as a function of distance, corresponding to a spectral singularity seated at $\alpha_2 = -3\pi/2$ with $a = 1$. See text.

value, $s = 5$, one finds four complex poles seated on the second quadrant of the $k$ plane. In general, for a spectral singularity with $s = m$ there will be $m - 1$ complex poles located on the second quadrant of the $k$ plane.

### C. Resonant states

Here we discuss briefly some features of the resonant functions for the absorptive case. The normalization of the resonant states follows by inserting the solution along the internal interaction in (58) into the normalization condition given by (10). The result yields, after some mathematical manipulation, using (59),

$$A_n = \left[\frac{2(-iba - 2i\kappa_n a)}{a(1 - iba - 2i\kappa_n a)}\right]^{1/2}. \tag{80}$$

Notice that in the limit $b \to \infty$, the normalization $A_n \to \sqrt{(2/a)}$, which corresponds to the trapped quantum states discussed above for an infinitely absorptive potential. For the spectral singularity resonant states where $\kappa_s = \alpha_s$ and substituting (79) into (80) the normalization condition $A_s$ reads

$$A_s = \left[\frac{-2i\alpha_s}{(1 - i\alpha_s a)}\right]^{1/2}. \tag{81}$$

From (58) one sees by continuity of the solutions at $r = a$ that $B_n = A_n \sin(\kappa_n a)\exp(-i\kappa_n a)$ and hence for $n = s$, using (81), allows one to calculate the spectral singularity resonant state.

Figure 3 exhibits a plot of the probability density of the spectral singularity resonant state as a function of distance for $s = 2$. Choosing $a = 1$, the intensity of the $\delta$ potential is $b_2 = 3\pi/2$ and hence the spectral singularity is located at $\alpha_2 = -3\pi/2$.

### D. Closure relationship for a test function

Here, we provide an example of Eq. (25) for the test function

$$F(r) = \sqrt{\frac{2}{a}}\,\sin(9\pi r/2a). \tag{82}$$

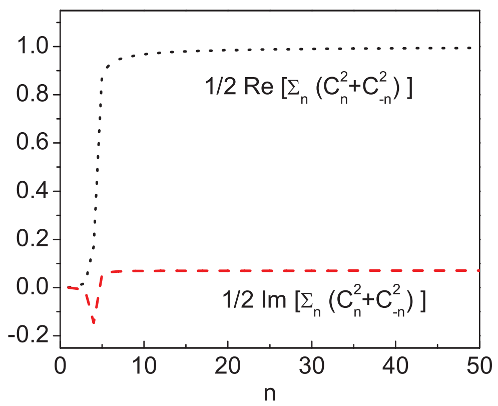

FIG. 4. (Color online) Plot of the real (dotted line) and imaginary parts (dashed line) of the closure relationship given by Eq. (25). See text.

Notice that this is not an infinite wall box function [50]. Since the test function is real, $C_n = \bar{C}_n$, we find it convenient to write Eq. (25) as

$$\frac{1}{2}\sum_{n=1}^{\infty}\left(C_n^2 + C_{-n}^2\right) = 1. \tag{83}$$

We obtain a set of poles $\{\kappa_n\}$ and resonant states $\{v_n\}$ for the $\delta$-shell potential given by Eq. (57) with parameters $b = 9\pi/2$ and $a = 1$ and then calculate the coefficients $C_n^2$, using (24), to evaluate (83). Notice that the above value of the intensity, in view of (79), corresponds to a *spectral singularity* at $s = 5$. An interesting consequence of this choice is that the real and imaginary parts of the coefficient $C_{-5}^2$ are, respectively, close to unity and to a vanishing value. In fact, the overlap of the test function with the rest of resonant states is very small.

Figure 4 yields a plot of both the real part of the left-hand side of (83) (dotted line) and the corresponding imaginary part (dashed line) as functions of the number $n$ of poles. One sees already that 50 poles satisfy to a good approximation the closure relationship given by Eq. (83).

### E. Emission case

As mentioned at the beginning of this section, the case for emission corresponds to the $\delta$-shell potential

$$U(r) = i\mathcal{W}(r) = ib\delta(r - a), \tag{84}$$

where $b > 0$. It then follows using Eq. (46) that the trajectories and distribution of the poles for the emission case may be obtained directly from those of the absorptive case by reflection with respect to the imaginary $k$ axis. For example, the case of the distribution of poles for a fixed value of the intensity of the $\delta$ potential depicted in Fig. 2 for $b = 9\pi/2$ becomes the distribution displayed in Fig. 5. It is worthwhile to note that for emission there appear poles that seat on the first quadrant of the $k$ plane. One sees that the spectral singularity is located at $\alpha_5 = 9\pi/2$. In general, for emission we have

$$\alpha_s = b_s. \tag{85}$$

The normalization condition for emission may be easily obtained. It gives the same expression as (81).

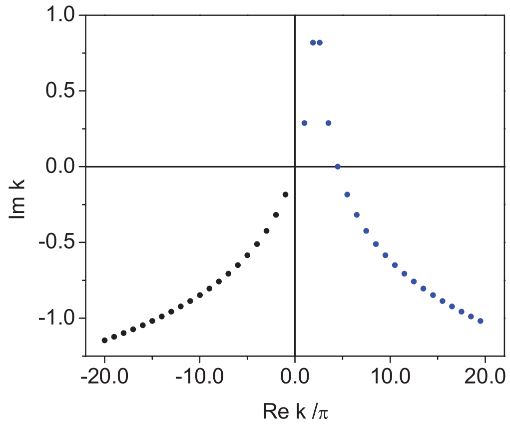

FIG. 5. (Color online) Plot of the distribution of the first 20 complex poles on the $k$ plane, corresponding to the purely emissive $\delta$-shell potential $U(r) = ib_s\delta(r-a)$, with $b_5 = 9\pi/2$ and $a = 1$, which yields a spectral singularity at $\alpha_5 = b_5$. See text.

### F. Resonant spectra for absorption and emission

For real potentials the quantity $|\mathbf{S}(k)|^2 = 1$ due to flux conservation. However, for purely imaginary potentials, $|\mathbf{S}(k)|^2$ yields information on the resonant structure of the system. Indeed, using the $\delta$-shell potential discussed above, let us first consider the distribution of poles for the absorptive case displayed in Fig. 2, which corresponds to $b_5 = 9\pi/2$ and $a = 1$. Figure 6 provides the corresponding plot of $|\mathbf{S}(k)|^2$ vs $k/\pi$. One observes a series of peaks, with maxima of unity value, that are closely related to the positions corresponding to the resonance poles, $a_r \approx n\pi$. At these peak values the flux is conserved. We have no explanation for the distinct values attained by the observed minima of $|\mathbf{S}(k)|^2$. It is not difficult to figure out the behavior of the absorptive cross section, which is defined as [51]

$$\sigma(k) = \frac{\pi}{k^2}\left[1 - |\mathbf{S}(k)|^2\right]. \qquad (86)$$

One sees that the peak values of $|\mathbf{S}(k)|^2$ correspond to vanishing values of $\sigma(k)$. This refers to situations where the continuum wave solution (41) behaves as the free solution, i.e., as if there were no potential at these values of $k$.

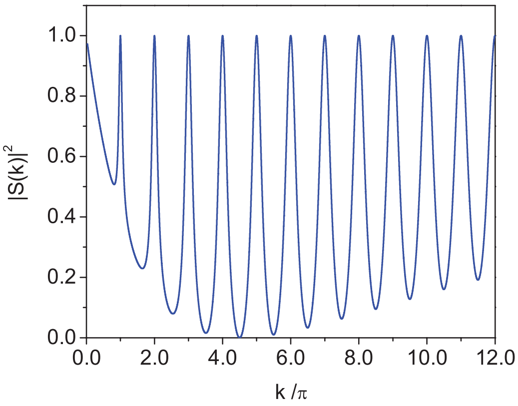

FIG. 6. (Color online) Plot of the function $|\mathbf{S}(k)|^2$ for the absorptive $\delta$-shell potential vs $k$ in units of $\pi$, with the same parameters as in Fig. 2. See text.

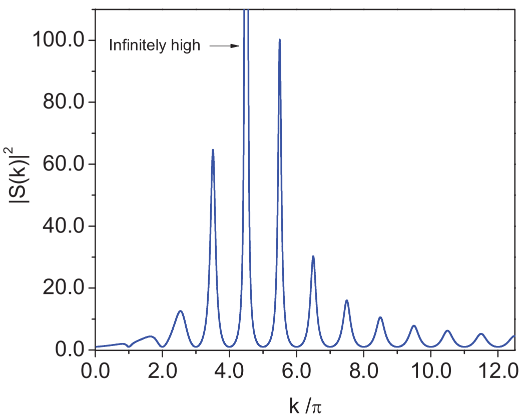

FIG. 7. (Color online) Plot of the function $|\mathbf{S}(k)|^2$ for the emission $\delta$-shell potential vs $k$ in units of $\pi$, with the same parameters as in Fig. 5. See text.

Another interesting feature appearing in Fig. 6 is that at $k/\pi = 4.5$, i.e., at $k = 9\pi/2$, the value of $|\mathbf{S}(k)|^2 = 0$. It is not difficult to see that this is the signature of the *spectral singularity* $\kappa_5 = -9\pi/2$ as shown in Fig. 2. This follows from Eq. (44), which informs us that for the case of a spectral singularity of $\mathbf{S}(k)$ situated at $-\kappa_s$ there corresponds a zero seated at $\kappa_s$. Using Eq. (86) one sees that for this case $\sigma(k = 9\pi/2) = 4/(81\pi)$, which says that the *spectral singularity* for absorption does not produce a singular behavior in the absorptive cross section.

The case for emission is displayed in Fig. 7. One observes also a peaked behavior of $|\mathbf{S}(k)|^2$ as a function of $k/\pi$. The most relevant feature of Fig. 7 is that $|\mathbf{S}(k)|^2$ attains an infinite value at $k/\pi = 4.5$ which corresponds precisely, as follows from inspection of Fig. 5, to the spectral singularity pole seated at $\kappa_5 = 9\pi/2$. The other peak maxima are related to the poles seated both on the first and fourth quadrants. All poles are close to the positions $a_r = (2n+1)\pi/2$. Notice that the four peaks situated on the left of the spectral singularity peak correspond, respectively, to the four poles seated on the first quadrant of the $k$ plane. For emission, the peak maxima of $|\mathbf{S}(k)|^2$ do not correspond to unity values as occurs for the case of absorption, but rather, to the minimum values occurring at $k/\pi = n$. We have no explanation for this nor for the distinct values of the peak heights except for the one that corresponds to the spectral singularity. Notice that in this case Eq. (86) yields negative values, which indicates that this expression is not suitable for emission.

It follows by inspection of Eq. (61) that as $k \to \infty$, $|\mathbf{S}(k)|^2 \to 1$. The former case is consistent with Sec. IV A1, which says that unitarity is restored for asymptotically large poles. Figure 8 yields a plot of $|\mathbf{S}(k)|^2$ vs $\log_{10} k$ for the absorption case that exhibits the behavior mentioned above for $b = 9\pi/2$ and $a = 1$. Similarly, Fig. 9 yields the corresponding behavior for the emissive case. The above figures exemplify that unitarity is restored far away from the region where $k \sim b$. This behavior holds in general for arbitrary finite range imaginary potentials.

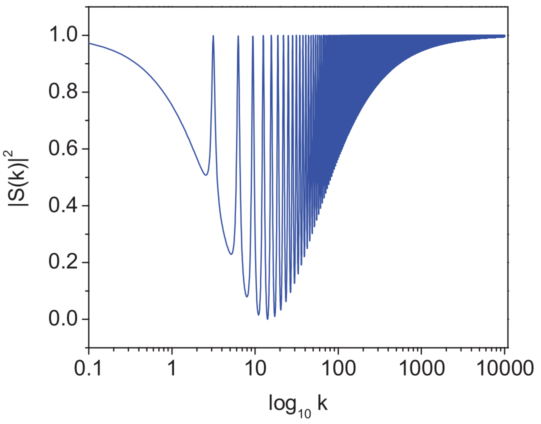

FIG. 8. (Color online) Plot of the function $|\mathbf{S}(k)|^2$ vs $\log_{10} k$ for the absorption $\delta$-shell potential with the same parameters as in Fig. 2. See text.

## V. CONCLUDING REMARKS

It is worth emphasizing Eqs. (35) and (38), which, as a consequence of the continuity equation, establish a general relationship between resonant states and spectral singularities, respectively, for absorption and emission. Notice that this result is independent of whether or not there is a real part in the potential. The effect of a real potential lies in the resonant functions. Another result worth emphasizing is the resonant expansion of the continuum wave solution in terms of resonant states given by Eqs. (49) and (55), respectively, along the internal and external interaction regions and similarly for the expressions of the continuum wave functions near a *spectral singularity* given by (50) and (56). Another result that deserves to be highlighted is that the residue at the pole of the outgoing Green's function corresponding to a spectral singularity is a well-defined function, contrary to the continuum wave function, which is not defined there. This might be of interest because for real potentials, the solutions to the time-dependent Schrödinger equation in terms of resonant states give exactly the same results as that involving continuum wave functions [52]. This implies that the formalism of resonant states might provide answers of physical interest where continuum wave functions are not defined and might also stimulate work towards a deeper understanding of the relationship between resonant and continuum states. A final remark refers to the exact numerical calculation of $|\mathbf{S}(k)|^2$ for the $\delta$-shell potential as a function of $k$. Our analysis shows, in general, that for absorption the *spectral singularity* [a pole of $\mathbf{S}(k)$] is seated on the negative imaginary $k$ axis that corresponds to a zero at $k = \alpha_s$ on the positive $k$ axis, as illustrated in the plot of $|\mathbf{S}(k)|^2$ shown in Fig. 7. However, for emission, the *spectral singularity* seats on the positive imaginary $k$ axis and hence it leads to an infinite value of $\mathbf{S}(k)$ as displayed in the plot of $|\mathbf{S}(k)|^2$ shown in (Fig. 8).

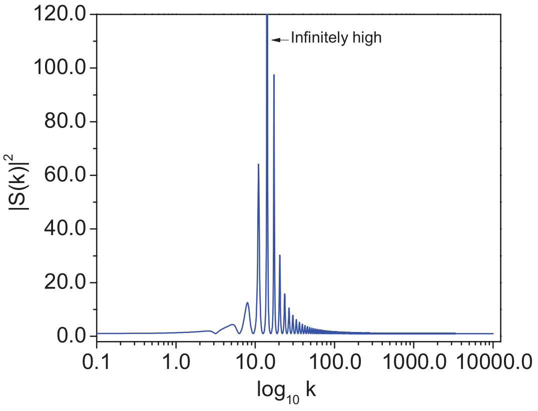

FIG. 9. (Color online) Plot of the function $|\mathbf{S}(k)|^2$ vs $\log_{10} k$ for the emissive $\delta$-shell potential with the same parameters as in Fig. 5. See text.

## ACKNOWLEDGMENT

G. García-Calderón acknowledges partial financial support form DGAPA-UNAM under Grant No. IN103612.

## APPENDIX A: DETERMINATION OF THE RESIDUE AT A POLE OF THE OUTGOING GREEN's FUNCTION FOR A COMPLEX POTENTIAL

Near a pole $\kappa_n$, in general, one may write the outgoing Green's function $G^+(r,r';k)$ as

$$G^+(r,r';k) \approx \frac{r_n(r,r')}{k-\kappa_n} + \chi(r,r';k), \tag{A1}$$

where $\chi(r,r';k)$ is a regular function of $k$. Substitution of (A1) into (1) yields

$$\begin{aligned} &\frac{1}{k-\kappa_n}\{r_n''(r,r') + [k^2 - U(r)]r_n(r,r')\} \\ &\quad + \{\chi''(r,r';k) + [k^2 - U(r)]\chi(r,r';k)\} \\ &\quad - (2m/\hbar^2)\delta(r-r') = 0. \end{aligned} \tag{A2}$$

Addition and subtraction of $\kappa_n^2 r_n(r,r')/(k-\kappa_n)$ into the above equation and taking the limit $k \to \kappa_n$ yields the expressions

$$r_n''(r,r') + \left[\kappa_n^2 - U(r)\right]r_n(r,r') = 0, \tag{A3}$$

and

$$\begin{aligned} &\chi''(r,r';\kappa_n) + \left[\kappa_n^2 - U(r)\right]\chi(r,r';\kappa_n) \\ &\quad + 2\kappa_n r_n(r,r') = (2m/\hbar^2)\delta(r-r'). \end{aligned} \tag{A4}$$

A similar procedure for the boundary conditions (2), after adding and subtracting $i\kappa_n r_n(r,r')/(k-\kappa_n)$ and taking the limit $k \to \kappa_n$, yields

$$r_n(0,r') = 0 \tag{A5}$$

and

$$\chi(0,r';\kappa_n) = 0, \tag{A6}$$

and, similarly,

$$r_n'(a,r') = i\kappa_n r_n(a,r') \tag{A7}$$

and

$$\chi'(a,r';\kappa_n) = i\kappa_n\chi(a,r';\kappa_n) + i r_n(a,r'). \tag{A8}$$

One sees, from (11), (12), (A3), (A5), and (A7), that both $v_n(r)$ and $r_n(r,r')$ satisfy the same equation and the same boundary conditions, which implies that they are proportional to each other, namely,

$$r_n(r,r') = v_n(r)P(r'). \tag{A9}$$

Using now Green's theorem between the equations for $v_n(r)$ and $\chi(r,r';\kappa_n)$, given respectively by (11) and (A4) gives

$$[v_n(r)\chi'(r,r';\kappa_n) - \chi(r,r';\kappa_n)v_n'(r)]_0^a + P(r')\int_0^a v_n^2(r)dr = (2m/\hbar^2)v_n(r'). \tag{A10}$$

It then follows using (12), (A6), (A8), and (A9) that

$$P(r') = (2m/\hbar^2)\frac{v_n(r')}{2\kappa_n\left\{\int_0^a v_n^2(r)dr + i v_n^2(a)/2\kappa_n\right\}}. \tag{A11}$$

Substitution of (A11) into (A9) finally gives the expression for the residue,

$$r_n(r,r') = (2m/\hbar^2)\frac{v_n(r)v_n(r')}{2\kappa_n\left\{\int_0^a v_n^2(r)dr + i v_n^2(a)/2\kappa_n\right\}}. \tag{A12}$$

Hence, provided the normalization condition is given by (10), one may write the residue at a pole $\kappa_n$ of the outgoing Green's function as displayed by (9).

## APPENDIX B: DERIVATION OF THE RESONANT EXPANSION OF $G^+(r,r';k)$

Consider the expression

$$\mathfrak{T} = \frac{1}{2\pi i}\int_C \frac{G^+(r,r';k')}{k'-k}dk', \tag{B1}$$

where $C$ is a large closed contour of radius $L$ in the $k'$ plane about the origin, as shown in Fig. 10, which excludes all the poles $\kappa_n$ and the value $k' = k$, namely, $C = C_R + c_k + \sum_n c_n$. Notice that $C_R$ is in the *clockwise* direction, whereas $c_k$ and the contours $c_n$ are in the *counterclockwise* direction. It follows using Cauchy's theorem that $\mathfrak{T} = 0$ and hence, using the theorem of residues to evaluate the distinct contours, one may write, in view of (9),

$$G^+(r,r';k) = (2m/\hbar^2)\sum_{n=-N}^{N}\frac{v_n(r)v_n(r')}{2\kappa_n(k-\kappa_n)} + \frac{1}{2\pi i}\int_{C_R}\frac{G^+(r,r';k')}{k'-k}dk'. \tag{B2}$$

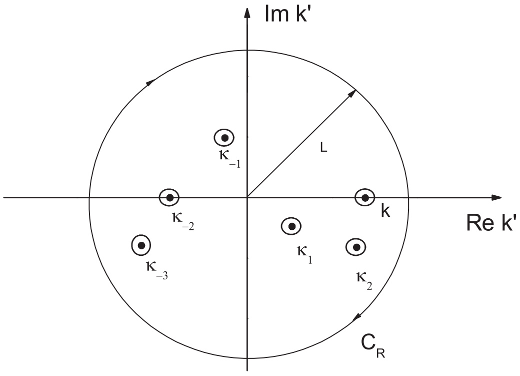

FIG. 10. Integration contour $C = C_R + c_k + \sum_n c_n$ used to obtain the resonant expansion of $G^+(r,r';k')$ in terms of the full set of complex poles. See text.

One may consider larger and larger values of the radius $L$, encompassing in that way more and more poles into the discrete sum in (B2). In the limit as $L \to \infty$, there will be an infinite number of terms in the sum. It turns out that on the complex $k'$ plane the outgoing Green's function

$$G^+(r,r';k') \to 0 \quad \text{as} \quad |k'| \to \infty, \tag{B3}$$

provided $r$ and $r'$ are smaller than the interaction potential radius $a$ and also for $r = a$ with $r' < a$ or vice versa. We denote these conditions by the notation $(r,r')^\dagger \leqslant a$. As a consequence, it follows that in the above limit the integral term in (B2) vanishes exactly and hence $G^+(r,r';k)$ may be expanded as the purely discrete resonant expansion given by Eq. (16). For values of $(r,r') \geqslant a$, $G^+(r,r';k')$ diverges in the limit $L \to \infty$ and therefore there is no purely discrete expansion of the outgoing Green's function in that case. The results, except that of Ref. [53], which refers only to values $(r,r') < a$, follow from the work of a number of authors [44,46,53,54]. It requires that the potential is of finite range, as considered in this work, or vanishes at infinite distance faster than exponential [40].

### 1. Example

Here we consider the exact analytical expression of the $s$ wave outgoing Green's function $G^+(r,r';k)$ for the $\delta$ potential model $V(r) = \lambda\delta(r-a)$, where the intensity $\lambda$ is a complex number. This makes it possible to verify that Eq. (B3) is fulfilled.

Our starting point is the expression for the outgoing Green's function given by Eq. (4), which is given in terms of the regular function, $\phi(k,r)$, the Jost function $f_+(k,r)$ and the Jost solutions. Choosing, $r < r'$ and $r' \leqslant a$, we find [23],

$$\phi(k,r) = \frac{\sin(kr)}{k}, \tag{B4}$$

$$f_+(k,r') = e^{ikr'} - \frac{\lambda}{k}\sin[k(r'-a)]e^{ika}, \tag{B5}$$

$$J_+(k) = 1 + \frac{\lambda}{k}\sin(ka)\,e^{ika}, \tag{B6}$$

and hence $G^+(r,r';k)$ may be written as

$$G^+(r,r';k) = -\frac{\sin(kr)}{k} \times \left[\frac{\exp(ikr') - (\lambda/k)\sin[\,k(r'-a)\,]\exp(ika)}{1 + (\lambda/k)\sin(ka)\exp(ika)}\right], \tag{B7}$$

where for the sake of simplicity we consider the units $\hbar = 2m = 1$.

Equation (B7) may be written, after a simple algebraic manipulation as

$$G^+(r,r';k) = -\frac{e^{ik(r+r')}}{B(k)} + \frac{e^{-ik(r-r')}}{B(k)} + \frac{\lambda e^{ik(r+r')}}{2ikB(k)} - \frac{\lambda e^{-ik(r-r')}}{2ikB(k)} - \frac{\lambda e^{ik(r-r')}e^{2ika}}{2ikB(k)} + \frac{\lambda e^{-ik(r+r')}e^{2ika}}{2ikB(k)}, \tag{B8}$$

where

$$B(k) = 2ik + \lambda[e^{2ika} - 1]. \tag{B9}$$

Recalling that $r < r'$, it is straightforward to see by inspection of each term in Eqs. (B8) and (B9) that along both the upper-half $I_+$ and the lower-half $I_-$ of the $k$ plane, where respectively, $k = \pm\alpha + i\beta$ and $k = \pm\alpha - i\beta$, $G^+(r,r';k)$ vanishes exponentially as $|k| \to \infty$ provided $(r + r') < 2a$. Clearly, also $(r - r') < 2a$. Similarly, along the real axis $G^+(r,r';k)$ vanishes at least as $1/k$. The above analysis holds also if $r' = a$.

[1] A. Mostafazadeh, Phys. Rev. Lett. **102**, 220402 (2009).

[2] A. A. Andrianov, F. Cannata, and A. V. Sokolov, J. Math. Phys. **51**, 052104 (2010).

[3] J. Dąbrowski, Phys. Rev. C **53**, 2004 (1996).

[4] N. A. Naimark, Trudy Moskow Mat. Obshch. **3**, 182 (1954); Am. Math. Soc. Transl. (2) **16**, 103 (1960).

[5] R. D. D. Kemp, Can. J. Math. **10**, 447 (1958).

[6] J. Schwartz, Commun. Pure Appl. Math. **13**, 609 (1960).

[7] A. Mostafazadeh and H. Mehri-Dehnabi, J. Phys. A **42**, 125303 (2009).

[8] B. F. Samsonov, J. Phys. A **38**, L397 (2005).

[9] A. Mostafazadeh, J. Phys. A **39**, 13495 (2006).

[10] A. Mostafazadeh, Phys. Rev. A **80**, 032711 (2009).

[11] Z. Ahmed, J. Phys. A: Math. Theor. **42**, 472005 (2009).

[12] S. Longhi, Phys. Rev. B **80**, 165125 (2009).

[13] A. Ruschhaupt, F. Delgado, and J. G. Muga, J. Phys. A **38**, L171 (2005).

[14] G. García-Calderón, Adv. Quantum Chem. **60**, 407 (2010).

[15] G. García-Calderón, AIP Conf. Proc. **1334**, 84 (2011).

[16] G. Gamow, Z. Phys. **51**, 204 (1928).

[17] G. Gamow, *Structure of Atomic Nuclei and Nuclear Transformations*, 2nd ed. (Clarendon Press, Oxford, 1937).

[18] A. F. J. Siegert, Phys. Rev. **56**, 750 (1939).

[19] J. Humblet and L. Rosenfeld, Nucl. Phys. **26**, 529 (1961).

[20] T. Berggren, Nucl. Phys. A **109**, 265 (1968).

[21] R. M. More and E. Gerjuoy, Phys. Rev. A **7**, 1288 (1973).

[22] R. de la Madrid, G. García-Calderón, and J. G. Muga, Czech. J. Phys. **55**, 1141 (2005).

[23] R. G. Newton, *Scattering Theory of Waves and Particles*, 2nd ed. (Dover, Mineola, NY, 2002), Chap. 12.

[24] G. García-Calderón and A. Rubio, Phys. Rev. A **55**, 3361 (1997).

[25] A. del Campo, G. García-Calderón, and J. Muga, Phys. Rep. **476**, 1 (2009).

[26] G. García-Calderón, J. L. Mateos, and M. Moshinsky, Phys. Rev. Lett. **74**, 337 (1995).

[27] G. García-Calderón, I. Maldonado, and J. Villavicencio, Phys. Rev. A **76**, 012103 (2007).

[28] S. Cordero, G. García-Calderón, R. Romo, and J. Villavicencio, Phys. Rev. A **84**, 042118 (2011).

[29] S. Cordero and G. García-Calderón, Phys. Rev. A **86**, 062116 (2012).

[30] R. de la Madrid, SIGMA **5**, 043 (2009).

[31] A. Bohm, M. Loewe, and B. V. de Ven, Fortschr. Phys. **51**, 551 (2003).

[32] R. de la Madrid, J. Phys A: Math. Gen. **39**, 9255 (2006).

[33] R. de la Madrid, J. Phys A: Math. Theor. **40**, 4671 (2007).

[34] S. Joffily, Nucl. Phys. A **215**, 301 (1973).

[35] W. J. Romo, Can. J. Phys. **52**, 1603 (1974).

[36] W. Cassing, M. Stingl, and A. Weiguny, Phys. Rev. C **26**, 22 (1982).

[37] G. García-Calderón and A. Rubio, Phys. Rev. B **46**, 9784 (1992).

[38] G. García-Calderón and L. Chaos-Cador, Phys. Rev. B **73**, 195405 (2006).

[39] J. G. Muga, J. P. Palau, B. Navarro, and I. L. Egusquiza, Phys. Rep. **395**, 357 (2004).

[40] H. M. Nussenzveig, *Causality and Dispersion Relations* (Academic Press, New York, 1972), Chap. 5.

[41] W. Schützer and J. Tiomno, Phys. Rev. **83**, 249 (1951).

[42] N. G. van Kampen, Phys. Rev. **91**, 1267 (1953).

[43] P. Exner and M. Fraas, J. Phys. A: Math. Theor. **40**, 1333 (2007).

[44] G. García-Calderón, Nucl. Phys. A **261**, 130 (1976).

[45] G. García-Calderón and A. Rubio, Nucl. Phys. A **458**, 560 (1986).

[46] G. García-Calderón and B. Berrondo, Lett. Nuovo Cimento **26**, 562 (1979).

[47] S. Cordero and G. García-Calderón, J. Phys. A: Math. Theor. **43**, 415303 (2010).

[48] S. Cordero and G. García-Calderón, J. Phys. A: Math. Theor. **44**, 305302 (2011).

[49] N. G. De Bruijn, *Asymptotic Methods in Analysis* (Dover, Mineola, NY, 1981).

[50] G. García-Calderón, J. L. Mateos, and M. Moshinsky, Ann. Phys. **249**, 430 (1996).

[51] M. A. Preston, *Physics of the Nucleus* (Addison-Wesley, Boston, 1962), Chap. 16.

[52] G. García-Calderón, A. Máttar, and J. Villavicencio, Phys. Scr., T **151**, 014076 (2012).

[53] R. M. More, Phys. Rev. A **4**, 1782 (1971).

[54] W. Romo, J. Math. Phys. **21**, 311 (1980).